Neutron scattering studies of structural phase transitions at Brookhaven*

G. Shirane

Brookhaven National Laboratory, Upton, New York 11973

Systematic neutron scattering studies on phase transitions have been carried out at Brookhaven in recent years. A consistent picture has now emerged from these investigations of "how" certain structural phase transitions take place. These are caused by a lattice dynamical instability; namely, the frequency of a particular lattice vibrational mode tends toward zero as the transition temperature is approached from above. At the transition these displacements are incorporated into the new atomic positions of the low-temperature phase. Modes of this type have become known as "soft" modes. This concept of soft modes was first emphasized by Cochran in 1960 for the special case of the $BaTiO_3$-type ferroelectrics. We have demonstrated that the generalized concept applies to many other types of structural phase transitions such as $SrTiO_3$(110°K), Nb_3Sn, SiO_2 and ND_4Br. The neutron scattering technique has been particularly useful in obtaining detailed knowledge of dynamical properties near the phase transition. This is due to a fortunate combination of the wavelength of typical thermal neutrons (2.5 Å) and their energy (13 meV). The phase transition studies, in turn, have contributed to considerable improvement of the inelastic neutron scattering technique, which may offer many future applications.

CONTENTS

I. INTRODUCTION

This is essentially a review of systematic neutron scattering studies of phase transitions, carried out for the past several years at the Brookhaven High Flux Beam Reactor. It may be appropriate to look back and reassess what was known about phase transitions in general at the outset. Limiting ourselves to phase transitions in solids, magnetic and superconducting transitions were already reasonably well understood. However, there were a large variety of other phase transitions in solids, investigated with different motives, and their various microscopic mechanisms appeared to be unrelated to each other. These included ferroelectrics, antiferroelectrics and still others such as SiO_2 and Nb_3Sn. All of these have been the subject of our systematic studies, and they became known as "structural" phase transitions. We have demonstrated that these transitions possess a simple and unified mechanism of a soft mode, namely a lattice dynamical instability.

In order to present this concept, let us first consider the well established case of magnetic phase transitions. A simple antiferromagnetic phase transition is caused by spin correlation due to exchange J_{ij}. Approaching the Néel temperature from above, the inverse staggered susceptibility χ_s^{-1} approaches zero; then at the transition the antiparallel spin configuration is formed with the familiar order parameter of sublattice magnetization M_s. A variety of magnetic phase transitions can be treated as generalizations of this basic mechanism. Because of this simplicity, the study of cooperative phenomena in magnetic systems has achieved considerable success, theoretically and experimentally.

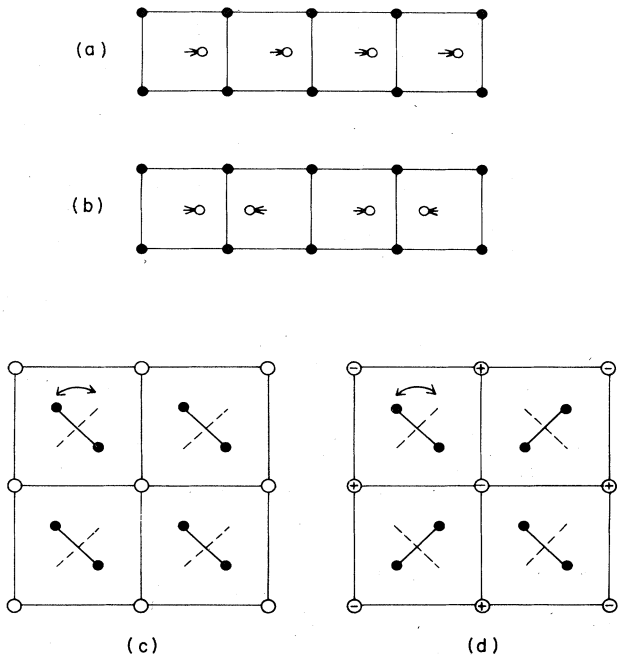

FIG. 1. Examples of atomic shifts in structural phase transitions. Here (a) and (b) are simplified versions of displacive transitions in perovskites, (c) order-disorder transition in ND_4Cl, (d) coupled mode of ND_4 and Br($\pm$ represents Br motion out of plane; see Fig. 15). The amplitude of the atomic shift Q_0 is the order parameter for the displacive transition.

The soft mode concept brings a similar unified picture to structural phase transitions in solids. In Fig. 1 we depict four examples of atomic shifts involved in structural phase transitions. They represent atomic positions in the ordered phases below the transition temperature T_c. Figures 1(a)

* Work performed under the auspices of the U.S. Atomic Energy Commission. This article is based on the talk given by Dr. Shirane on the occasion of his receiving the Oliver E. Buckley Solid State Physics Prize at the meeting of the American Physical Society in San Diego, March 1973.

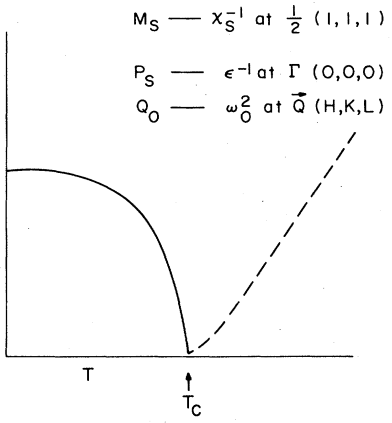

FIG. 2. Schematic comparison of order parameter and inverse susceptibility for different types of phase transitions. M_s; sublattice magnetization, P_s; spontaneous polarization, Q_0; atomic displacement in the structural transition.

and 1(b) are simplified versions of the perovskite-type structure, and they are both derived from the symmetric high-temperature phase. The arrows in these figures correspond to an atomic vibrational motion of a single normal phonon mode; (a) the transverse optic (TO) mode at $\mathbf{q} = 0$, and (b) the zone boundary mode which creates a doubling of the unit cell. A displacive phase transition results when one of these vibrational modes becomes unstable; namely, the phonon frequency ω_0 tends towards zero. At the transition temperature T_c this "soft phonon" motion freezes into the static displacement of the low-temperature phase. The amplitude of this shift Q_0 is the order parameter (see Fig. 2), and ω_0^2 corresponds to the inverse susceptibility. (See Cochran, 1969, and Axe, 1971.)

This is essentially the model first proposed by Cochran and also by Anderson in 1960 for the $BaTiO_3$-type ferroelectrics. It was later extended to KH_2PO_4 and $NH_4H_2PO_4$ by Cochran (1961) and to the zone boundary instability in perovskites by Cochran and Zia (1968). Our systematic neutron scattering studies have demonstrated that the generalized soft mode concept covers the essential mechanism of phase transitions in solids. We show schematically the typical soft mode phase transitions in Fig. 3 and some details are listed in Table I, which summarize our neutron scattering experiments.

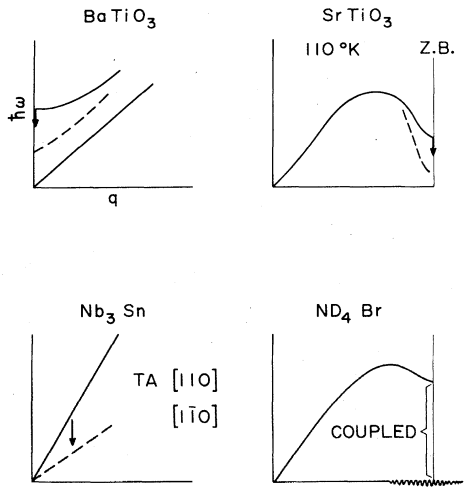

FIG. 3. Typical soft mode (arrows) phase transitions studied at Brookhaven. These represent temperature-dependent phonon dispersion relations $\hbar\omega$ vs $\mathbf{q}$.

The examples in Fig. 3 depict two very important characteristics of soft modes, which are shown by arrows in the figure. The first point is the location of the soft modes in the reciprocal space. This can be described by the total momentum transfer $\mathbf{Q}$, which is related to the Bragg positions $2\pi\boldsymbol{\tau}$ (= $\mathbf{G}$) by

$$\mathbf{Q}(HKL) = 2\pi\boldsymbol{\tau}(hkl) + \mathbf{q} = \mathbf{G} + \mathbf{q}, \tag{1}$$

where H, K, and L may take nonintegers, and $\mathbf{q}$ represents the wave vector of the soft phonon. In addition to the Γ point ($\mathbf{q} = 0$) for ferroelectrics such as $BaTiO_3$, the soft mode condensation may take place at zone boundaries or in a transverse acoustic (TA) branch. It is by no means easy to locate the soft mode; actually this is the main problem for neutron scattering experiments, since it is basically a very time-consuming research tool (see Sec. II).

The second feature is shown in the last example of Fig. 3, ND_4Br. Now we are introducing the additional freedom of

TABLE I. Lattice dynamical phase transitions investigated by neutron scattering at the Brookhaven High Flux Beam Reactor. They are classified according to the location of soft modes; ZC (zone center), ZB (zone boundary), TA (transverse acoustic). Here C is central symmetric; P, piezoelectric, F, ferroelectric

Soft mode	Symmetry	Crystal	T_c	References
ZC	F–C	$PbTiO_3$	490°C	Shirane *et al.* (1970)
	F–C	$BaTiO_3$	130°C	Yamada, Shirane, Linz (1969). Shirane *et al.* (1970) Harada, Axe, Shirane (1971)
	F–C	$KTaO_3$	<0°K	Shirane, Nathans, Minkiewicz (1967). Axe, Harada, Shirane (1970) Comès, Shirane (1972)
	F–C	$KNbO_3$	420°C	Nunes, Axe, Shirane (1971)
	F–P	KD_2PO_4	220°K	Skalyo, Frazer, Shirane (1970)
	P–P	SiO_2	573°C	Axe and Shirane (1970)
ZB	C–C	$LaAlO_3$	535°C	Axe, Shirane, Muller (1969) Kjems *et al.* (1973)
	C–C	$SrTiO_3$	110°K	Shirane, Yamada (1969) Shapiro *et al.* (1972)
	C–C	$KMnF_3$	186°K	Minkiewicz, Shirane (1969) Shirane, Minkiewicz, Linz (1970) Gesi *et al.* (1972)
	P–P	$ND_4D_2PO_4$	240°K	Meister *et al.* (1969)
	F–P	$Tb_2(MoO_4)_3$	160°C	Dorner, Axe, Shirane (1972)
	C–C	ND_4Br	215°K	Yamada *et al.* (1974)
TA	C–C	Nb_3Sn	46°K	Shirane, Axe (1971) Axe, Shirane (1973)

tunneling or order–disorder motion (see the bottom of Fig. 1). As shown by Kobayashi (1968) for KD_2PO_4, this tunneling motion may couple with a lattice vibrational mode. Here, the order–disorder motion of ND_4 is coherently coupled with the Br motion. This is probably the simplest example of coupled modes, and there will be many interesting examples to be investigated in the future. Thus we include in structural phase transitions both *displacive* and *order–disorder* types of phase transitions. I prefer the term "lattice dynamical" phase transitions, but the shorter term "structural" is now more widely used.

Once we locate the soft mode, then the important characteristics can be elucidated, limited only by experimental accuracies. Figure (2) depicts order parameter Q_0 measured *below* T_c, and the corresponding soft mode energy $\hbar\omega_0$ measured *above* T_c. The latter follows approximately

$$(\hbar\omega_0)^2 = A(T - T_0). \tag{2}$$

Using these we can express the free energy as

$$F = \tfrac{1}{2}\omega_0^2 Q_0^2 + \cdots + \tfrac{1}{2}cu^2. \tag{3}$$

For the well known case of ferroelectrics, the order parameter Q_0 corresponds to spontaneous polarization P_s, and the inverse susceptibility to reciprocal dielectric constant ϵ^{-1}, as schematically shown in Fig. 2. The second term comes from strain u, and this coupling of u and Q_0 plays a very important role in structural phase transitions. This is one very distinct difference from the magnetic case where magnetoelastic interaction usually plays the secondary role.

This paper is not intended to be a comprehensive and balanced review of recent studies of structural phase transitions. Rather, it views the problem entirely from the angle of neutron scattering. For the other aspects of this very active field, readers may refer to review articles by Cochran (1969), Cowley and Coombs (1973), and Blinc and Zeks (1972).

II. NEUTRON SCATTERING TECHNIQUE

Among many experimental techniques used to study phase transitions, neutron scattering occupies a unique position as a very powerful and very slow tool at the same time. Figure 4 illustrates this point. Shown here are phonon dispersion relations for successive Brillouin zones. Here **Q** represents the total momentum transfer as defined in Eq. (1). The dynamical properties of solids can be characterized by measuring the scattering function $S(Q, \omega)$ for an appropriate range of **Q** and energy $\hbar\omega$. There are three scattering techniques available for this purpose: light, x-ray and neutron scattering. Raman scattering offers extremely high accuracy and a wide range of energy, but it can cover only a very narrow range of **Q**. X-ray scattering on the other hand suffers from poor energy resolution so that one cannot observe phonons directly.

The neutron scattering can cover a wide range of **Q** (*many* Brillouin zones) with modest energy resolution, as sketched in Fig. (4). This is due to a fortunate energy–wave vector relation for thermal neutrons; for example, 13 meV–2.5 Å^{-1}. The wave vector **k** has an amplitude $2\pi/\lambda$, and this determines the range of **Q** to be covered. Another important

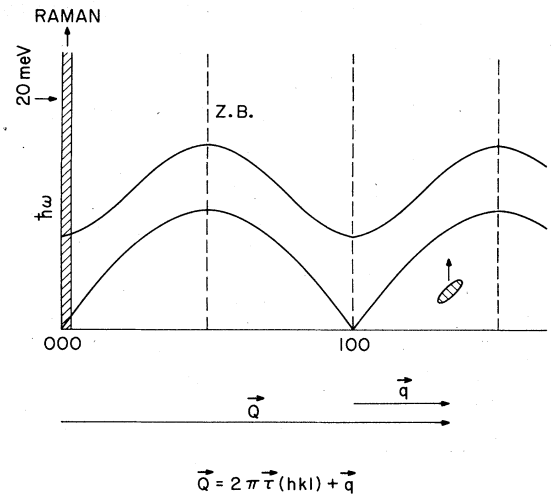

FIG. 4. Comparison of Raman and neutron scattering techniques. Resolution function is depicted by an ellipsoid with arrow indicating constant **Q** scan. Here 1 meV = 8.1 cm^{-1} = 11.6°K.

advantage of neutron scattering comes from the fact that phonons are always coupled to neutron waves. On the other hand many soft phonons, in particular above T_c, are Raman inactive. This is the reason that our studies have centered on the high-temperature phase.

We take advantage of two important features shown in Fig. 4. The first is of course the direct observation of phonon energy and line shape near the phase transitions. The second is the intensity measurements of equivalent **q** phonons in various Brillouin zones as described in Sec. VI. We may emphasize that the frequencies repeat, but intensities do not, from one Brillouin zone to the other.

We have used exclusively triple-axis spectrometers and the constant **Q** technique. This was invented by Brockhouse in 1961, and it is the simplest and the most powerful method for the study of crystalline solids. As schematically shown in Fig. 4, this technique allows us to keep **Q** vectorially constant. This is essential in most of the measurements in crystals, and it has now become the standard way to study elementary excitations in solids. The available neutron sources give "modest" intensities for inelastic scattering resulting from the inherent inefficiency of this type of spectrometer. Neutron energy is determined by Bragg reflections by monochromator and analyzer, before and after the sample scattering. Therefore the resolution in the ω–q space is relatively poor. Thus it is extremely important to have exact knowledge of the resolution function of a given spectrometer. Concentrated effort along this line has been pursued by Nathans and many others at Brookhaven. The first comprehensive account of this topic was given by Cooper and Nathans (1967).

In recent years remarkable progress has been made in the efficient use of low-energy neutrons (below 50 meV). This is due to the advent of pyrolytic graphite crystals, developed by Union Carbide Corporation. They have extremely high reflectivity, particularly below 20 meV (~2 Å in λ). Moreover, the bent graphite can effectively focus neutron beams as discussed by Riste (1970) and Nunes and Shirane (1971). In addition, the graphite can also be used as an extremely efficient filter for higher orders at 14 meV (see Shirane and

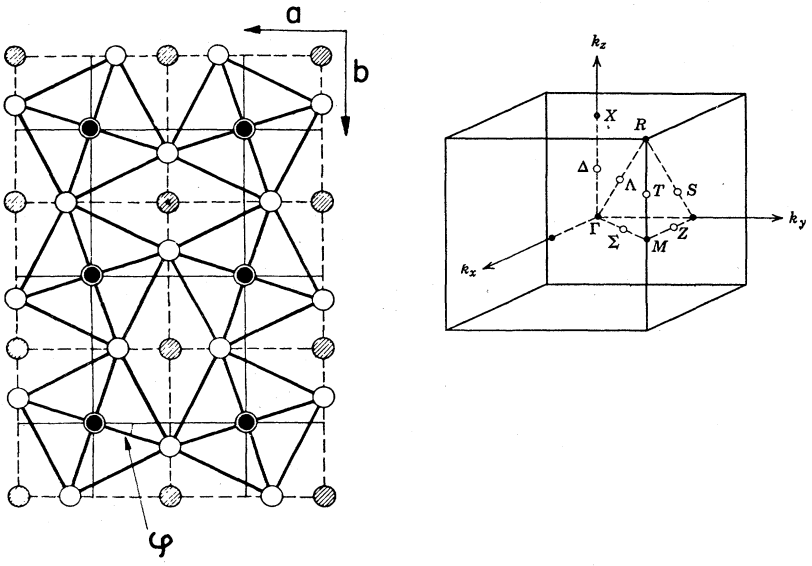

FIG. 5. The low temperature structure proposed by Unoki and Sakudo (1967) is shown on the left-hand side. They demonstrate the rotation of the oxygen octahedron surrounding Ti. The right-hand side shows the reciprocal space, in particular R and M points with the origin again at Γ.

Minkiewicz, 1970, and Shapiro and Chesser, 1972). It is now possible to obtain a much stronger and cleaner neutron beam at 14 meV. This energy, together with a Be filtered beam below 5 meV, offers an almost ideal tool for the study of phase transitions. Moreover, the phonon cross sections are proportional to $T \times \omega_0^{-2}$, where ω_0 for the soft mode approaches zero at the transition. The smallest crystal investigated so far is Nb_3Sn, with a volume of 0.05 cc.

III. $SrTiO_3$ (110°K)

This phase transition is probably the simplest example of a structural phase transition. As we have already shown in Fig. 3, it is due to a zone boundary soft mode and it was the first example of this kind. In part due to the availability of large single crystals from National Lead Company, this phase transition has now become most extensively studied. Another advantage of this transition is its second-order character. In contrast to the magnetic cases there are not many displacive type phase transitions which are truly of the second order, as this one is.

Historically, this phase transition had been known for many years, and several models were proposed without success. At 110°K, where the elastic constants show rather significant change, *no* anomaly was observed for the dielectric constant. This latter can be checked quite accurately because $SrTiO_3$ is a well known incipient ferroelectric with $T_c \sim 0$°K and the dielectric constant shows a very steep temperature dependence following the Curie–Weiss law, $\epsilon^{-1} = (T - T_0)/C$. The cubic lattice constant shows a small splitting ($<0.1\%$) to a tetragonal distortion. No information was available from x-ray diffraction concerning the atomic shifts through the 110°K phase transition. Then Unoki and Sakudo (1967) proposed a low-temperature structure based on their ESR measurements. They deduced the structure shown on the left-hand side of Fig. 5. This suggestion was made into a concrete model by Fleury, Scott and Worlock (1968). They interpreted their Raman spectrum *below* 110°K based upon the model that the Γ_{25} phonon at this R point, namely the [111] zone boundary, softens as the temperature decreases to 110°K. This specific model follows logically if the Unoki-Sakudo structure is the consequence of a soft mode instability.

The direct evidence of a soft phonon at the R point was provided by the inelastic neutron experiment of Shirane and Yamada (1969). Their results are shown in Fig. 6. At the transition the zone boundary becomes a superlattice point, enlarging the unit cell. It was shown that the soft mode energy $\hbar\omega_0$ follows closely (see Fig. 7)

$$(\hbar\omega_0)^2 = A(T - T_0)^\gamma \tag{4}$$

with $\gamma \sim 1.0$. The more recent experiment by Shapiro *et al*

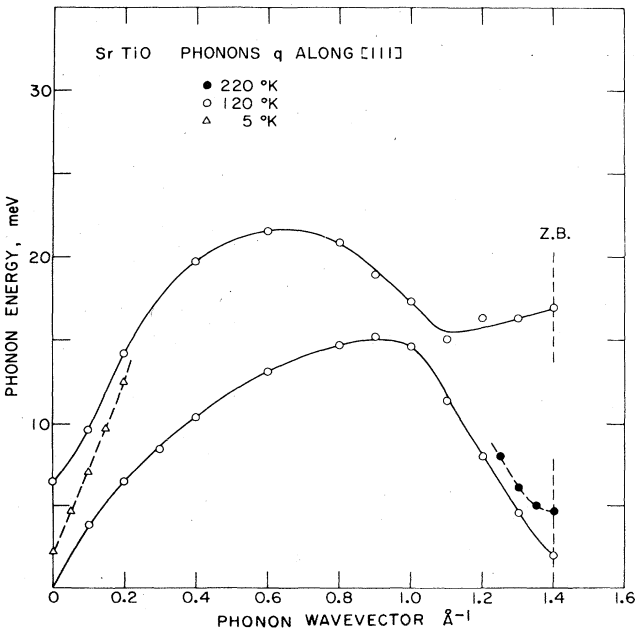

FIG. 6. Temperature-dependent phonon modes in $SrTiO_3$ measured by Shirane and Yamada (1969). The 110°K transition is caused by the soft mode at the zone boundary. Soft mode near the origin is due to incipient ferroelectricity.

(1972) indicates γ is larger than one, in accordance with the order parameter exponent $\beta = 0.33$ determined by Müller and Berlinger (1971).

The neutron experiment shows that the soft mode corresponds to a very simple rotation of oxygen octahedra as depicted in Fig. 5. The octahedra on the layer above rotate the opposite way. The structure shown here also corresponds to a static structure of the low-temperature phase. One can see there is only one parameter ϕ, the rotation angle, which is the order parameter of the phase transition. This is, of course, related linearly to the oxygen shift Q_0. The relation between the soft mode motion and the condensed structure was discussed by Cochran and Zia (1968) in a more general context. It is important to recognize that the low-temperature phase of $SrTiO_3$ represents the condensation of a *single* normal mode of vibration. Arbitrary atomic shifts of course do *not* satisfy this condition.

IV. $KMnF_3$

We have just demonstrated a simple lattice dynamical phase transition in $SrTiO_3$ due to rotational instability of the oxygen octahedron. It has since been shown that this is a very common mechanism of phase transitions in many perovskite type compounds, such as $LaAlO_3$, $NaNbO_3$ and $CsPbCl_3$ (see Table I). Here $KMnF_3$ offers a particularly interesting example. In addition to its antiferromagnetic Néel temperature $T_N = 88°K$, this crystal exhibits two successive phase transitions, at 186° and 91°K. This is somewhat analogous to the well known case of ferroelectric $BaTiO_3$ where cubic–tetragonal–orthorhombic–rhombohedral transitions were accounted for by Devonshire's phenomenological theory (1954). The spontaneous polarization changes direction in an "appropriate" sequence. These successive phase transitions are quite instructive in giving additional information on the stability of atomic arrangement.

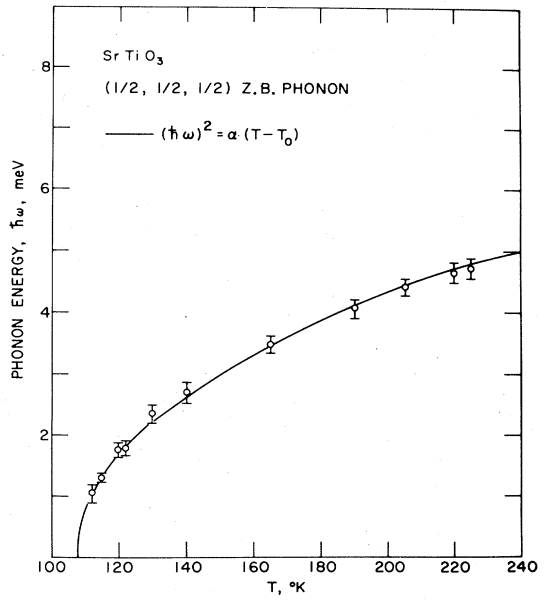

FIG. 7. Soft phenon energy $\hbar\omega$ in $SrTiO_3$ approaching the 110°K transition. After Shirane and Yamada (1969).

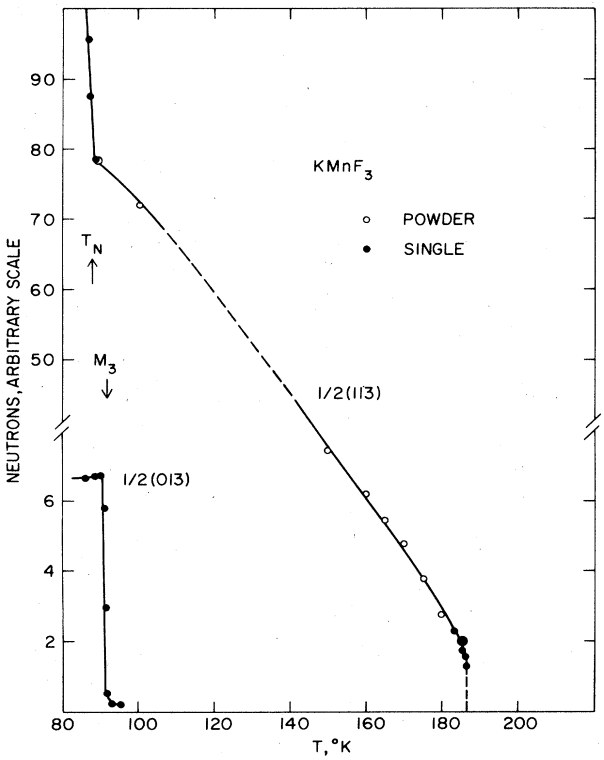

FIG. 8. The temperature dependence of the Bragg intensities for the Γ_{25} and M_3 structural transitions and the Néel temperature in $KMnF_3$. After Shirane, Minkiewicz, and Linz (1970).

As shown in Fig. 8 the two successive transitions in $KMnF_3$ both involve zone boundary instabilities. The first phase transition at 186°K is identical to the $SrTiO_3$ (110°K) R point instability (the Γ_{25} mode). Then it is followed by the condensation of the M_3 mode at the [110] zone boundary, the M point. These two soft modes are very simply related as one can see in Fig. 5. The Γ_{25} mode at the R point corresponds to the octahedra rotation in opposite directions in successive layers, thus resulting in $\frac{1}{2}(111)$ momentum transfer. On the other hand, the M_3 mode at the $\frac{1}{2}(110)$ zone boundary represents the rotation in the same direction in all layers, thus *not* doubling the unit cell along the tetragonal c direction.

The octahedra rotation mode between R–M has very special properties; namely, the only parameter is the rotation angle between successive layers. Gesi *et al.* (1972) examined this branch by mounting the $KMnF_3$ crystal in a special fashion. As shown in Fig. 9, the phonon modes between M and R all have low energies and are completely flat at room temperature. This branch first lowers uniformly on cooling; then approaching 186°K, the R point mode tends to condense, and at lower temperature the M point mode softens. This corresponds to a rodlike diffuse x-ray scattering observed by Comès *et al.* (1971).

One can look upon the situation as a strong two-dimensional coupling within the layer perpendicular to the rotation axis. Here the analogy to a two-dimensional antiferromagnet, K_2NiF_4, is quite obvious. (See Birgeneau, Skalyo, and Shirane, 1970.) The magnetic case is of course simpler because we have usually only one spin wave dispersion

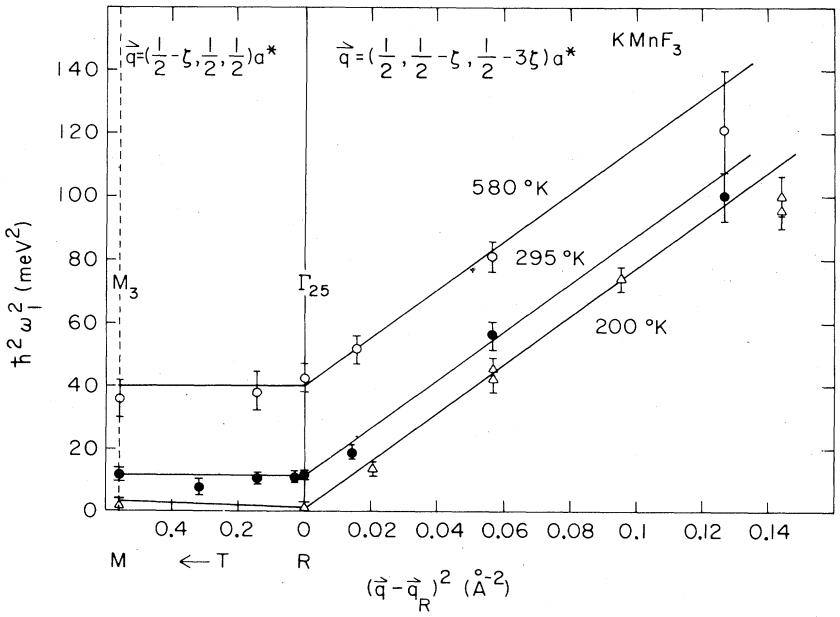

FIG. 9. Phonon dispersion relation through R and M points (see Fig. 5) in $KMnF_3$, after Gesi *et al.* (1972). The flatness between R and M indicates the strong two-dimensional correlation. The scale ($\hbar\omega^2$) vs q^2 was used because of its convenient linear relation for optic modes.

curve. The lattice dynamical case is inherently more complicated because there is much more freedom of motion as represented by multiple phonon branches. One can demonstrate, however, that the instantaneous correlation of rotational fluctuation is influenced by each phonon with its ω^{-2} factor. Thus the low-lying modes dominate, creating a two-dimensional model as shown in Fig. 5.

V. $KTaO_3$

The original concept of soft modes was proposed for ferroelectrics, namely a soft mode at $\mathbf{q} = 0$, and the pioneering neutron scattering study of a soft mode was carried out by Cowley for $SrTiO_3$ in 1964. Since then, very extensive measurements have been made on several perovskites, ABO_3, as shown in Table I. In contrast to the zone boundary soft mode, the ferroelectric soft mode is much more difficult to study by neutron scattering, because at the limit of $h\omega \to 0$, $q \to 0$, they overlap with the Bragg peak. Thus it is not possible to single out the soft mode alone as demonstrated in the previous sections for $SrTiO_3$ and $KMnF_3$. Among the several perovskites studied, $KTaO_3$ offers the cleanest example even though the Curie temperature is not realized above 0°K; thus it is an incipient ferroelectric. The unique characteristic of $KTaO_3$ is its underdamped (well defined) soft optic mode compared with the cases of $BaTiO_3$ and $KNbO_3$. Another example of an underdamped optic soft mode is $SrTiO_3$ ($T_c \sim 0$°K); this case is complicated, as we know now, because of the preceding zone boundary transition at 110°K.

The temperature dependence of the soft transverse optic mode in $KTaO_3$ was measured by Shirane, Nathans, and Minkiewicz in 1967. They showed that the relation

$$(\hbar\omega_0)^2 = A \times \epsilon^{-1} \tag{5}$$

is followed very closely in this crystal for a wide temperature range. The soft mode is well defined down to 4°K, and this made the observation very definitive. In other ferroelectrics, such as $BaTiO_3$ and $KNbO_3$, the high damping of the soft mode made the proper characterization much more difficult.

Further study of $KTaO_3$ was carried out by Axe, Harada, and Shirane (1970) and their results revealed a rather remarkable phonon coupling in this crystal. As shown in

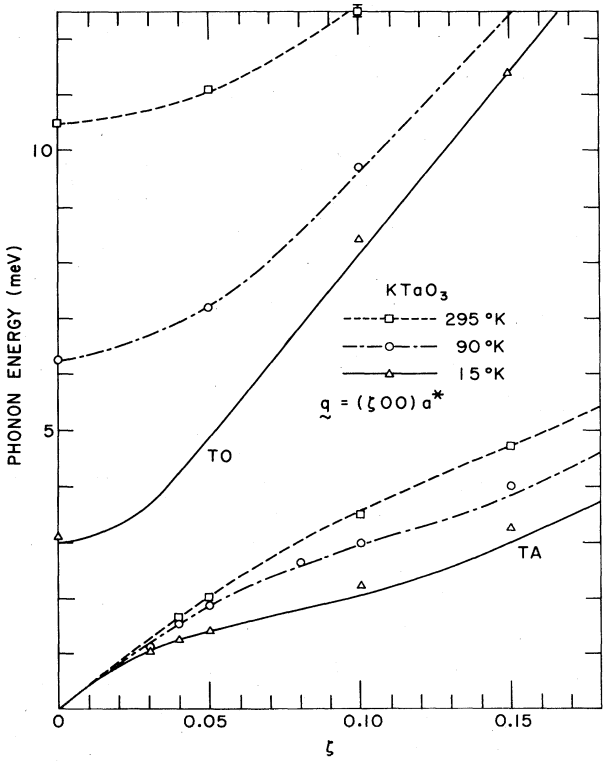

FIG. 10. Transverse optic (TO) and transverse acoustic (TA) phonon coupling in $KTaO_3$ as reported by Axe, Harada, and Shirane (1970). The lines represent a simple model fit as explained in the original paper.

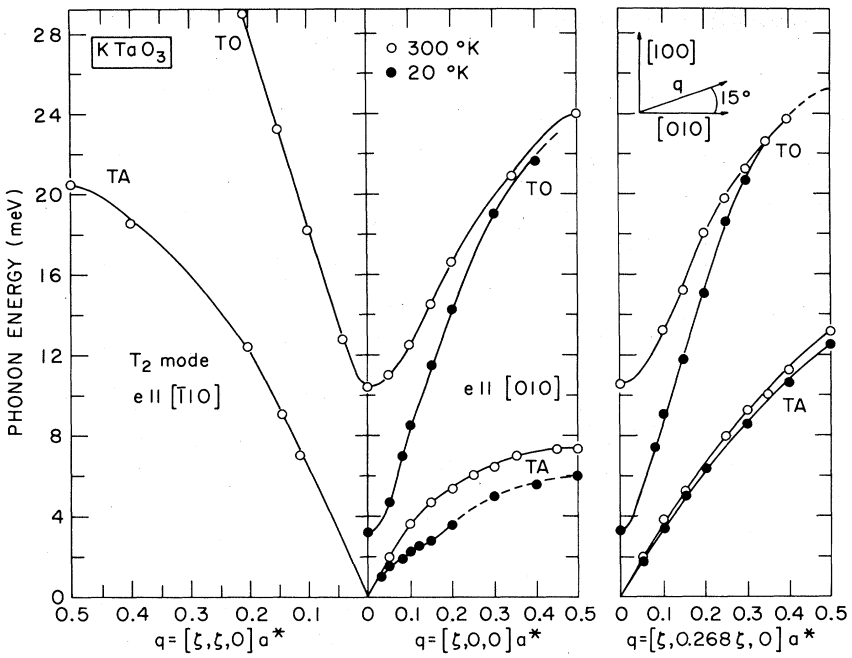

FIG. 11. Dispersion relation in $KTaO_3$ for different directions and temperatures, studied by Comès and Shirane (1972). Note the strong TA dip only along [100].

Fig. 10, the very dramatic change was observed in the *acoustic* branch at finite q's. At low temperature this branch shows a clear dip, but the limiting slope at $q = 0$ is temperature-independent in agreement with ultrasonic measurements. In addition, very strong anomalies were noted for the neutron cross sections of the TO and TA phonons as a function of temperature. All of these observations were explained as the result of coupling of optic- and acousticlike excitations. In centrosymmetric crystals, this interaction vanishes as $\mathbf{q} \rightarrow 0$. This is a typical example of a soft mode permitting us to study very interesting interactions rarely observable otherwise. The unique interpretation is often possible because of their temperature and directional dependence.

Another interesting aspect of $KTaO_3$ is the strong directional dependence of its phonon dispersion curve. This is shown in Fig. 11, taken from the measurements of Comès and Shirane (1972). The [100] branch (center) is essentially the overall view of Fig. 10. The right-hand side figure depicts the dispersion curves taken 15° off the [100] (see insert). We note here that the TA branch is almost temperature independent; namely, the TO–TA coupling is unusually strong only along the [100] direction. More generally, it was shown that both the TA and TO phonons polarized along [010] have particularly low frequencies in the reciprocal {100} sheets, though it is not easily seen from Fig. 11 alone. Only in these sheets is the TO–TA coupling remarkably enhanced.

We have just described the "dip" in phonon frequency in the {100} reciprocal sheets. Since the intensities of phonons are proportional to $1/\omega^2$, these dips appear as a strong x-ray diffuse scattering on {100} reciprocal sheets, as reported by Comès *et al.* (1968) for several perovskites. Physically, this anisotropic dispersion relation is a result of strong dipole–dipole coupling along the ⟨100⟩ directions, as discussed first by Slater in 1950 and more recently by Hüller (1969). Namely, if the correlation is strong in the ⟨100⟩ directions, the Fourier transform in the reciprocal lattice consists of lower energy phonons in the {100} sheets. Here again the similarity with one-dimensional antiferromagnet is striking.

It is likely that this strong one-dimensional correlation is the basic characteristic in many other perovskite-type ferroelectrics as our extensive studies (see Table I) have indicated for $BaTiO_3$, $KNbO_3$, and $PbTiO_3$. In $KTaO_3$, this point has been most clearly demonstrated.

VI. MODE DETERMINATION

Once we establish the location and temperature dependence of the soft mode, the next question is what are the atomic motions involved in this soft mode and how are they related to the atomic positions in the low-temperature phase? The first serious effort along this line was by Harada, Axe, and Shirane (1970) on $KTaO_3$ and other perovskites. As shown in Fig. 4, we are now taking advantage of the fact that thermal neutrons can cover several Brillouin zones in contrast to the Raman scattering. The intensity of inelastic scattering for a one-phonon process is proportional to the square of the inelastic structure factor (see Cochran 1969). Here

$$F(\text{phonon}) = \sum_k (\mathbf{Q}\cdot\boldsymbol{\xi}_k) b_k \exp(i\mathbf{G}\cdot\mathbf{r}_k), \tag{6}$$

where $\mathbf{Q} = \mathbf{G} + \mathbf{q}$ as defined in Eq. (1), b_k is the neutron scattering length for kth atom, with mass m_k and coordinate $\mathbf{r}_k$. The displacement vector $\xi_k(\mathbf{q}, j)$ for phonons in jth branch is related to the atomic displacement $\mathbf{u}_{kl}$ for kth atom in lth cell and the polarization vector $\mathbf{e}_k(\mathbf{q}, j)$ by

$$u_{kl}(t) = (Nm_k)^{-1/2} \sum_{\mathbf{q},j} \mathbf{e}_k(\mathbf{q}, j) Q(\mathbf{q}, j; t) \exp(i\mathbf{q}\cdot\mathbf{r}_{kl}), \tag{7}$$

$$\boldsymbol{\xi}_k = (m_k)^{-1/2} \mathbf{e}_k. \tag{8}$$

The amplitude Q_0 of the normal coordinate Q of the soft

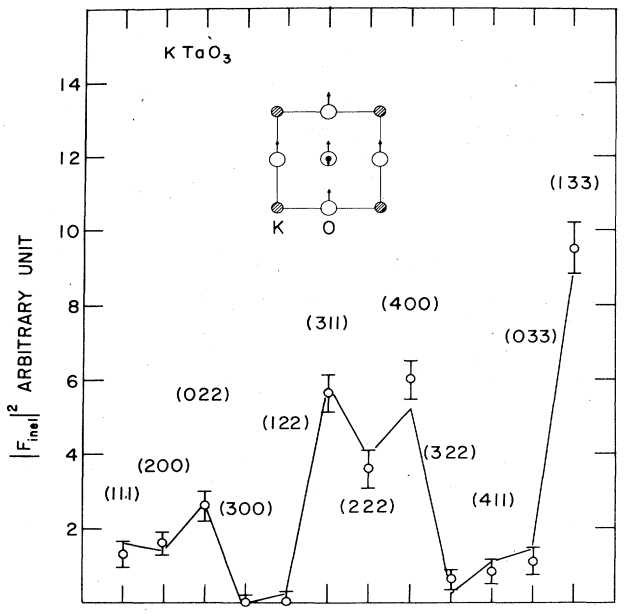

FIG. 12. Mode determination of ferroelectric TO phonon in $KTaO_3$, after Harada, Axe, and Shirane(1970). The solid line represents calculated values for the Slater mode as shown in the insert.

phonon is the order parameter of the transition as we have discussed in Sec. I.

Conceptually, this mode determination is very similar to the conventional structure determination where the elastic structure factor for Bragg reflections is given by

$$F(\text{Bragg}) = \sum_k b_k \exp(i\mathbf{G}\cdot\mathbf{r}_k). \tag{9}$$

Here $\mathbf{r}_k$'s are unknown, whereas in Eq. (6) $\boldsymbol{\xi}_k$'s are to be determined. The importance of mode determination had been recognized previously, but weak phonon intensities in general presented considerable difficulty. Soft modes offered an almost ideal opportunity to develop the basic technique for this "dynamical crystallography" since the phonon intensity is proportional to ω_0^{-2}.

The first example of our effort along this line is shown in Fig. 12 for the $\mathbf{q} = 0$ ferroelectric mode in $KTaO_3$. This was essentially a two-parameter fit and excellent agreement was obtained (solid line in the figure) assuming only the Slater-type motion, namely the oxygen octahedron moving as a unit against Ta as shown by the insert. This experiment has established the feasibility of the mode determination technique; it has since been applied successfully to several other cases.

In the simplest case of the $SrTiO_3$ 110°K transition, in which only one parameter (rotation angle ϕ) is involved, the mode determination reduces to an almost trivial case. Nevertheless, it is important to visualize that the low-temperature phase corresponds to the "freezing in" of the soft mode motion above T_c. Generally speaking, the "difference" of static structures above and below T_c roughly corresponds to the soft mode motions. We have demonstrated this for several crystals shown in Table I. One can then question whether mode determination is necessary when both structures are known. The answer is no, *if* one is convinced that the particular phase transition is caused by a soft mode. In magnetism no one cares to determine the magnetic structure by studying the intensity modulation of the critical scattering above T_N. The next example sheds light on the interesting difference between magnetic and lattice dynamical phase transitions.

Figure 13 shows the *static* structure of ferroelectric $PbTiO_3$ at room temperature which was determined in 1956 before the soft mode concept was proposed. This crystal is similar to $BaTiO_3$ and $KNbO_3$ but it has much larger atomic shifts. Its soft mode was shown by Shirane *et al.* (1970) to be well defined (not overdamped) despite its high Curie temperature of 490°C. Again the soft mode motion corresponds to the atomic shifts through the transition.

The point we would like to make is that these "shifts" *cannot* be deduced uniquely without invoking the soft mode concept. The left-hand side of Fig. 13 depicts the structure with the conventional origin at Pb. It was argued that the magnitude of shift δ's depends on an arbitrary choice of Pb position as the origin; it may be more natural, then, to refer to the unshifted oxygen octahedron. We may recall an unending discussion, before 1960, on what atom did "move" through phase transitions in $PbTiO_3$ and other perovskites. From the viewpoint of the soft mode, this is unique since an optic phonon at $\mathbf{q} = 0$ must satisfy the simple condition that the center of mass is not displaced, namely

$$\sum m_j \boldsymbol{\xi}_j = 0. \tag{10}$$

This results in the shifts shown on the right side of Fig. 13 and these are actually the mode motions displayed by the soft modes, as determined recently by Shirane *et al.* (1970). This shows a considerable shift of Pb in contrast to $KTaO_3$.

Another very interesting example of the zone center soft mode is the α–β quartz transition at 573°C. As shown in Fig. 14, this mode is Raman inactive in the high-temperature phase and thus can be investigated only by neutron scattering. The mode determination by Axe and Shirane (1970) demonstrated again that the soft mode motions correspond

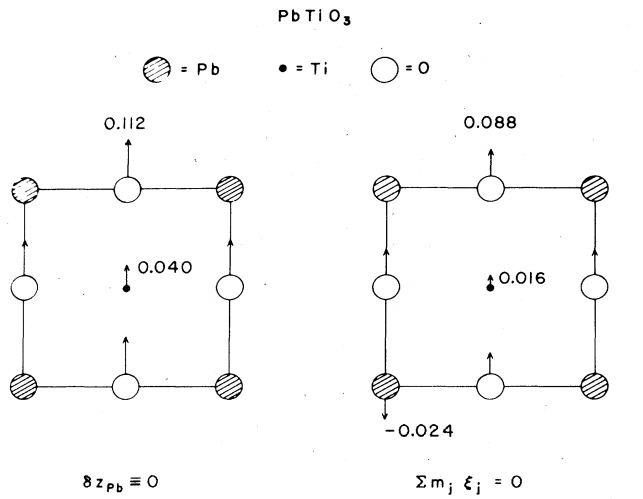

FIG. 13. Static crystal structure of tetragonal $PbTiO_3$ determined by Shirane, Pepinsky, and Frazer (1956) shown with two different origins. The numbers given are in units of c.

to the static displacement pattern previously determined by x-rays. In this crystal the zone center soft mode is heavily damped but it can be easily separated out from the sharp Bragg peak.

We have so far considered only displacive type phase transitions. In addition, some order-disorder type phase transitions can be attributed to coupled phonon-tunneling modes. The best known example is KD_2PO_4, for which Kobayashi (1968) has formulated a successful theoretical model. Very recently, the phase transition of ND_4Br at 215°K was investigated by Yamada *et al.* (1974). This may represent one of the simplest coupled modes and the mode determination by neutron scattering plays a key role in establishing the nature of phase transitions. The ordered structure below T_c is shown in Fig. 15 and the "projection" of the enlarged unit cell in Fig. (1d). Above T_c, the ND_4 ions in the center are disordered; that is, they take one of two equivalent positions (90° rotation).

This configuration in ND_4Br may be called antiparallel; the alternative ordering scheme is the parallel one as shown in Fig. (1c) and observed in ND_4Cl. A microscopic aspect of this transition and its dynamical characteristics are treated theoretically by Yamada *et al.* (1972 and 1973). Their model emphasizes the coherent coupling of the ND_4 flipping to the Br vibrational motion as shown in Fig. 15. The scattering cross section for this coupled motion is shown schematically in Fig. 3 as a "triple peak" structure along the [110] direction. The central (quasielastic) component is due to the coupled relaxation motion of the Br displacement and the ND_4 flipping. This was directly proved by neutron intensity distribution among various [110] zone boundaries.

In addition, we observe a well defined TA phonon mode at the [110] zone boundary which corresponds to Br motion shown in Fig. 15, and this is also the spontaneous displacement in the low-temperature phase. This phonon mode around 7 meV is noticeably broadened by the coupling. The strong temperature dependence, however, is centered in the quasielastic component. This corresponds to the slow relaxation case where the ND_4 flipping is slow compared with

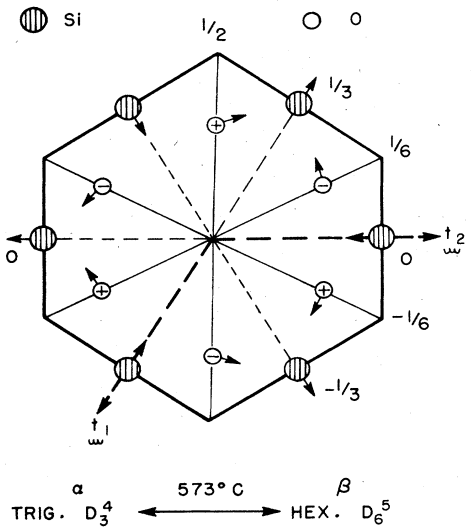

FIG. 14. A projection on the basal plane of β quartz. The arrows indicate the shifts in atomic positions between the β phase and the room temperature α phase. After Axe and Shirane (1970).

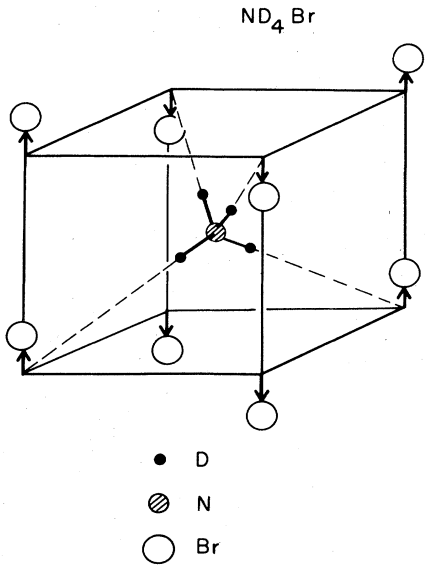

FIG. 15. Coupled mode in DN_4Br studied by Yamada *et al.* (1974). The displacements of Br^- ions are coupled coherently to ND_4^+ flipping into 90° positions.

the Br vibration. In the other extreme case of fast relaxation, the phonon side bands show a critical softening.

VII. CLASSIFICATION OF PHASE TRANSITIONS

We have now shown that lattice instability is the basic mechanism of the displacive phase transitions; we then extended the concept by including the order-disorder motion coupled to phonons. This encompasses most phase transitions in solids outside of magnetic and superconducting phase transitions. We now arrive at a logical way to classify the structural phase transitions first by the location of the soft mode, as was done in Table I for the crystals we have investigated. The first group possesses soft optic phonons at the zone center, and most of them are ferroelectric, except SiO_2 which we have discussed in some detail. These ferroelectrics have been very extensively investigated over the last twenty years because they reveal themselves by spontaneous polarization and diverging dielectric constants. Recent soft mode investigation gave a rather clear microscopic picture for the transitions. In addition, many interesting anharmonic effects due to phonon-phonon coupling have been discovered.

The second group, to which we paid most attention in this paper, show zone boundary instability. These are probably the most common phase transitions in solids and in their simplest form they resemble antiferromagnets. They can be subclassified by the symmetry of the phase above T_c and the degeneracy of the soft modes. In Table I we have used the notation C: centrosymmetric, P: piezoelectric and F: ferroelectric.

The most surprising example in this group is $Tb_2(MoO_4)_3$. This is an excellent example to demonstrate how the soft mode idea, once established, can resolve many puzzling features. This crystal is ferroelectric in the sense that it shows a reversible spontaneous polarization below T_0. However, the dielectric constant shows only a small anomaly

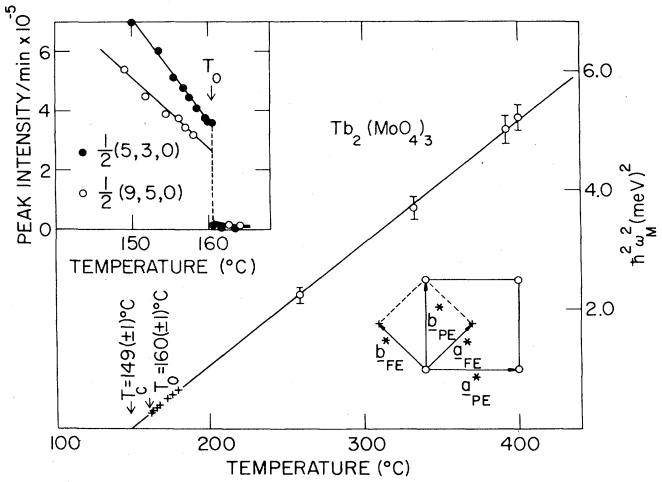

FIG. 16. Unexpected zone boundary soft mode for ferroelectric $Tb_2(MoO_4)_3$, reported by Dorner, Axe, and Shirane (1972). The relation between paraelectric (PE) and ferroelectric (FE) reciprocal lattices is shown in insert.

for an unclamped crystal and even this disappears when the crystal is clamped. Following a suggestion by Pytte (1970), a neutron scattering study by Dorner, Axe, and Shirane (1972) revealed soft mode behavior not in a $\mathbf{q} = 0$ polar phonon but at the M point, [110] zone corner of paraelectric (PE) phase. (See Fig. 16.)

In this case, the spontaneous polarization appears as a secondary effect because of the piezoelectric nature of the high-temperature phase. One can express the free energy in simplified form as

$$F = \tfrac{1}{2}\omega_M{}^2 Q_M{}^2 + \cdots + \tfrac{1}{2}cu^2 + \chi^{-1}P_z{}^2 + gQ_M{}^2 u + aP_z u. \tag{11}$$

By setting $\partial F/\partial P_z = \partial F/\partial u = 0$, we obtain

$$P_z = a\chi u, \tag{12a}$$

$$u = -(g/c)Q_M{}^2. \tag{12b}$$

Thus the spontaneous polarization P_z is a necessary consequence of its linear coupling to strain u. In this case, one does not expect an anomaly in susceptibility χ^{-1} at T_c because this is not the driving force of the transition. This crystal is an example of what is now occasionally called an "improper" ferroelectric.

The last example in Table I, Nb_3Sn, undergoes an acoustic phonon instability (see Fig. 3). This particular transition at 45°K has received considerable attention in connection with the high superconducting transition at 18°K; the relation between the two is still very much an open question. We may call this type of phase transition a generalized Jahn–Teller type, and it appears to be an active research topic for the near future.

Following are two topics which have a special significance in structural phase transitions.

A. Order parameter

At first glance, it may appear easy to identify the order parameter in a given phase transition. As we have shown, this is the first and quite often the most difficult task, in a study of structural phase transitions. In magnetic phase transitions, this problem is not even mentioned since it is so obvious. We have defined the order parameter Q_0 in conjunction with Eqs. (3) and (7). This Q_0 is nothing but the amplitude of the atomic displacements of the soft modes. Therefore once we identify the location and mode motion of a temperature-dependent soft mode, the order parameter is uniquely established. If, however, one starts with macroscopic properties such as spontaneous polarization, elastic constant, or lattice distortion, then the identification of the order parameter is sometimes quite difficult, as we know in typical examples of $SrTiO_3$ and $Tb_2(MoO_4)_3$.

First let us consider an obvious case, that of ferroelectric $BaTiO_3$. We can expand the free energy as

$$F = \tfrac{1}{2}\omega_0{}^2 Q_0{}^2 + \cdots + \tfrac{1}{2}cu^2 + dQ_0{}^2 u. \tag{13a}$$

In this case the reversal of the sign of atomic shifts does not change the free energy, thus $dQ_0{}^2u$ term (see Fig. 12). We obtain by $\partial F/\partial u = 0$

$$u = (d/c)Q_0{}^2. \tag{13b}$$

This tetragonal strain $u = (c/a - 1)$ is a secondary (driven) order parameter in contrast to a primary driving order parameter Q_0. This point was first brought into focus by Axe in 1971. In the case of $BaTiO_3$, it is trivial. In other cases like $Tb_2(MoO_4)_3$(TMO), this created considerable difficulty in establishing the true nature of phase transition. Since TMO is ferroelectric it was naturally assumed that the spontaneous polarization was the primary order parameter.

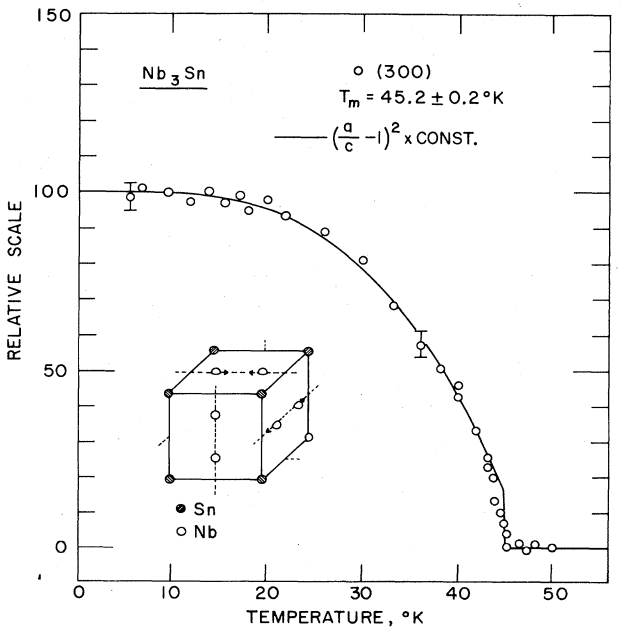

FIG. 17. Temperature dependence of intensity I of new Bragg peak (300) in Nb_3Sn. It shows $I \propto Q_0{}^2 \propto u^2$. Atomic displacements are shown in the insert. After Shirane and Axe (1971).

Here Nb_3Sn offers another interesting example. Shirane and Axe (1971) have shown that it is the [110] shear strain which corresponds to the primary order parameter, in agreement with the original Labbé–Friedel model (1966). This shear strain produces, by a linear coupling, Nb displacements and new Bragg reflections such as (300) shown in Fig. 17. The free energy now has the form

$$F = \tfrac{1}{2}\omega_0^2 Q_0^2 + \cdots + \tfrac{1}{2}cu^2 + gQ_0u. \tag{14a}$$

This gives

$$u = (g/c)Q_0. \tag{14b}$$

This linear term gQ_0u implies that displacements reverse signs if lattice distortion changes from $a/c > 1$ to $a/c < 1$. (This is more clearly seen if you shift the origin of the inset in Fig. 17 by $\frac{1}{2}a$ to the right.) This relation was experimentally verified as shown in Fig. (17). When two parameters, u and Q_0, are linearly related, then it is essentially a matter of taste which one to call the primary order parameter.

B. First-order transition

As we have seen, most of the structural phase transitions are of the first order. This is in contrast to the magnetic Curie or Néel points where the second-order nature is the rule rather than the exception. This, I believe, is the result of strong coupling between the order parameter (atomic shifts) and strain in structural phase transitions. It was shown by Devonshire (1954) that the first-order transition in $BaTiO_3$ at 130°C becomes second-order if the sample is kept at constant volume. In magnetic systems, the first-order phase change may be materialized by an exceptionally strong strain dependence of exchange forces.

Among the crystals listed in Table I, only $SrTiO_3$, and possibly $LaAlO_3$, show truly second-order nature. All others exhibit a finite discontinuity in the order parameter; however, they are characterized by large critical fluctuations as shown by soft phonons with decreasing ω_0. They are "nearly" second-order in this sense and we may define the degree of first order by $\delta_2 = \Delta T/T_c$ as shown in Fig. 18. This usually is small, of the order of a few percent. This means that the behavior very near the phase transition cannot be reached experimentally. On the other hand, this does not prevent us from studying the basic mechanisms of lattice dynamical instability. Another criterion used more often is $\delta_1 = \Delta Q_0/Q_0(0)$ (see Fig. 18), since this quantity is usually easier to measure. This value, however, depends sensitively on a particular model (or high orders in free energy expansions). Namely, δ_1 can be nearly one where δ_2 is quite small. The conspicuous example is Slater's celebrated model of KH_2PO_4 (1941), where $\delta_1 = 1$, and $\delta_2 = 0$, although this may be a very special case.

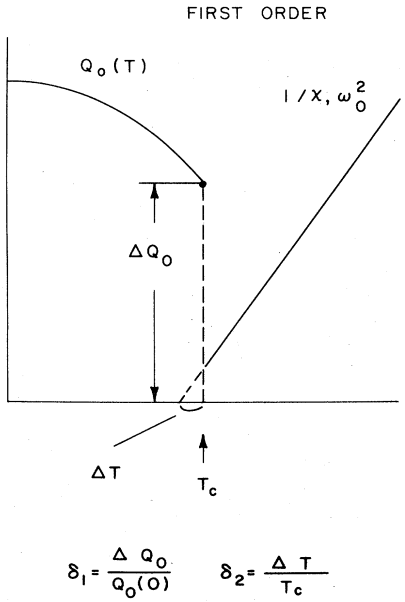

FIG. 18. Schematic showing a discontinuity of the order parameter Q_0 at a first order transition T_c.

The phase transitions between two ordered states are usually of first order. Typical examples are low-temperature phase transitions in $BaTiO_3$, and the M point transition in $KMnF_3$ at 91°K (see Fig. 8). From the very abrupt change of the order parameter at 91°K, it appears that this transition is strongly first order. On the other hand, if one measures appropriate fluctuations above the transition, the value of δ_2 is only 1.3% as shown by Shirane *et al.* (1970).

VIII. CONCLUDING REMARKS

We have demonstrated that the concept of soft mode provides the most fundamental mechanism of structural phase transitions in solids. This concept of soft mode has recently been applied, with various degrees of success, to a very wide range of topics including surface, magnetism, melting, and superconductivity. Let us compare again the structural phase transition with its magnetic counterpart in order to gain a proper perspective. As we have discussed previously, structural phase transitions are inherently much more complex. However, we have now established the basic mechanism, which is somewhat equivalent to the concept of anti- and ferrimagnetism developed by Néel some years ago. Namely, we now have the unified soft mode picture of "how" the phase transitions take place.

Concerning the details of critical phenomena, such as the critical exponents β and γ, only limited success has been achieved so far. Here we define $Q_0 = A'(T_0 - T)^\beta$ and $\omega_0^2 = A(T - T_0)^\gamma$. Theoretically and experimentally, this topic has been explored exhaustively for magnetic systems with great success. This is due to the relative simplicity of magnetic interactions, which occur in well characterized varieties such as Ising, Heisenberg, three and two dimensions.

As for the structural phase transitions, reliable data are scarce; this is due to the extreme sensitivity of the details of the transition to strain and impurity. (This is not so in magnetic systems.) One can see that strains are strongly coupled to the order parameter and this in turn makes most structural phase transitions slightly first order. Here $SrTiO_3$ is one of the exceptions and exhibits a truly second-order 110°K transition. Müller and Berlinger (1971) demonstrated $\beta \approx 0.33$ and recent neutron experiments by Shapiro *et al.* (1972) indicated that γ is larger than one. On the other hand, several ferroelectrics are known to behave

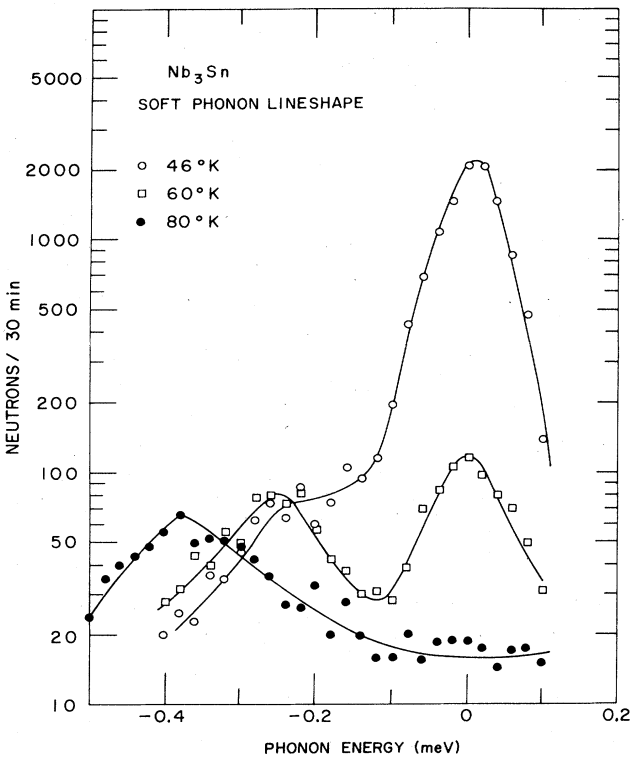

FIG. 19. Soft phonon line shape in Nb_3Sn observed by Axe and Shirane (1973). Negative energy corresponds to neutron energy gain. Notice the side band phonon and the central peak.

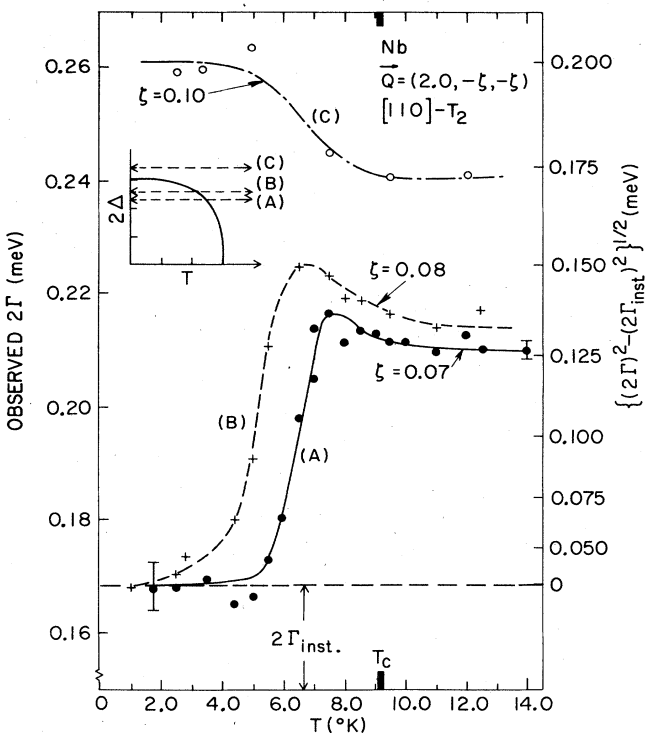

FIG. 20. Acoustic damping due to superconducting electron phonon interaction in Nb. Notice definite changes as phonon energies cut across energy gap 2Δ. After Shirane, Axe, and Shapiro (1973).

with classical exponents of $\beta = 0.5$ and $\gamma = 1.0$. This variance in behavior is not yet understood theoretically and remains one of the challenging problems in this field.

One very important byproduct of soft mode studies has been the demonstration of pronounced anharmonic effects near the transitions. The soft mode frequencies become very low and strongly temperature dependent, and this often permits a unique interpretation. One good example has already been discussed in Figs. 10 and 11, the strongly directional coupling of optic and acoustic branches in $KTaO_3$. Another dramatic effect takes place in the soft phonon line shapes, as shown in Fig. 19 for Nb_3Sn by Axe and Shirane (1973). These profiles show a very strong "central" peak in addition to phonon side bands. This unusual effect was first discovered near the 110°K transition in $SrTiO_3$ by Riste *et al.* (1971) and further investigated by Shapiro *et al.* (1972). Similar results observed in Nb_3Sn are somewhat better characterized due to a wider q width of the central peak. This central peak was phenomenologically interpreted as representing the difference between the zero and first sounds. The microscopic picture is not yet well understood and requires further theoretical studies.

Finally, I would like to emphasize that the structural phase transitions have been extensively investigated by many other experimental techniques. Inelastic neutron spectroscopy with constant Q technique is, nonetheless, almost ideally suited for the overall study of phase transitions. The soft mode experiments, in turn, have contributed to a considerable improvement of the technique. It is now possible to scan reliably intensities for a wide range of $S(Q, \omega)$ and to investigate an extremely small crystal through inelastic studies, e.g. Nb_3Sn with 0.05 cc in volume as shown in Fig. 19.

We believe that this high resolution neutron technique will find wide applications in studies of condensed matter. One such example is shown in Fig. 20 as the direct observation of electron–phonon interaction in superconducting Nb. The line broadening is suppressed when the phonon energy $\hbar\omega_p$ is less than the superconducting energy gap $2\Delta(T)$. Also clearly observed is the small "increase" of the interaction just above $2\Delta(T)$ line, and this is one of the features predicted by Bobetic (1964) using the BCS model. A similar study, though less accurate, was also carried out on Nb_3Sn and this revealed the strong directional dependence of the electron–phonon interaction due to superconductivity (Axe and Shirane, 1973).

This brief review is based on the talk given at the APS meeting, San Diego, March 1973. It is naturally not intended to be a comprehensive review of the topic. I wanted to demonstrate what kind of information is now obtainable by the advanced neutron scattering technique, not only for structural phase transitions but also for many other topics in solid state physics.

ACKNOWLEDGMENTS

These neutron scattering studies have been carried out at Brookhaven in collaboration with many of my colleagues, as can be seen in the references of Table I. It has been a series of exciting experiments full of surprises, and I am grateful to all of my colleagues for this very enjoyable collaboration. In particular, I would like to thank J. D. Axe and Y. Yamada for many illuminating discussions.

REFERENCES

Anderson, P. W., 1960, Fizika dielekrikov, G. I. Skanavi, Ed. Acad. Nuak SSSR, Mowcow, 290.
Axe, J. D., 1971, Trans. Am. Crystallogr. Assoc. **7,** 89.
Axe, J. D., J. Harada, and G. Shirane, 1970, Phys. Rev. B **1,** 1227.
Axe, J. D., and G. Shirane, 1970, Phys. Rev. B **1,** 342.
Axe, J. D., and G. Shirane, 1973, Phys. Rev. B **8,** 1965.
Axe, J. D., G. Shirane, and K. A. Müller, 1969, Phys. Rev. **183,** 820.
Birgeneau, R. J., J. Skalyo, Jr., and G. Shirane, 1970, J. Appl. Phys. **41,** 1303.
Blinc, R., and B. Zeks, 1972, Adv. Phys. **27,** 693.
Bobetic, V. M., 1974, Phys. Rev. **136,** A 1535.
Brockhouse, B. N., 1961, *Inelastic Scattering of Neutrons in Solids and Liquids* (Intern. Atomic Energy Agency, Vienna) 113.
Cochran, W., 1960, Adv. Phys. **9,** 387.
Cochran, W., 1961, Adv. Phys. **10,** 401.
Cochran, W., 1969, Adv. Phys. **18,** 157.
Cochran, W., and A. Ziz, 1968, Phys. Status Solidi **25,** 273.
Comès, R., F. Denoyer, L. Deschamps, and M. Lambert, 1971, Phys. Lett. **34A,** 65.
Comès, R., M. Lambert, and A. Guinier, 1968, Solid State Commun. **6,** 715.
Comès, R., and G. Shirane, 1972, Phys. Rev. B **5,** 1886.
Cooper, M. J., and R. Nathans, 1967, Acta Crystallogr. **23,** 357.
Cowley, R. A., 1964, Phys. Rev. **134A,** 981.
Cowley, R. A., and G. J. Coombs, 1973, J. Phys. C **6,** 143.
Devonshire, A. F., 1954, Adv. Phys. **3,** 85.
Dorner, B., J. D. Axe, and G. Shirane, 1972, Phys. Rev. B **6,** 1950.
Fleury, P. A., J. F. Scott, and J. M. Worlock, 1968, Phys. Rev. Lett. **21,** 16.
Gesi, K., J. D. Axe, G. Shirane, and A. Linz, 1972, Phys. Rev. B **5,** 1933.
Harada, J., J. D. Axe, and G. Shirane, 1970, Acta Crystallogr. **A26,** 608.
Harada, J., J. D. Axe, and G. Shirane, 1971, Phys. Rev. B **4,** 155.
Hüller, A., 1969, Z. Phys. **220,** 145.
Kjems, J. K., G. Shirane, K. A. Müller, and H. J. Scheel, 1973, Phys. Rev. B **8,** 1119.
Kobayashi, K. K., 1968, J. Phys. Soc. Jap. **24,** 497.
Labbé, J., and J. Friedel, 1966, J. Phys. Radium **27,** 153 and 303.
Meister, H., J. Skalyo, Jr., B. C. Frazer, and G. Shriane, 1969, Phys. Rev. **184,** 550.
Minkiewicz, V. J., and G. Shriane, 1969, J. Phys. Soc. Jap. **26,** 674.
Müller, K. A., and W. Berlinger, 1971, Phys. Rev. Lett. **26,** 13.
Nunes, A. C., J. D. Axe, and G. Shriane, 1971, Ferroelectrics **2,** 291.
Nunes, A. C. and G. Shriane, 1971, Nucl. Instrum. Methods **95,** 445.
Pytte, E., 1970, Solid State Commun. **8,** 2101.
Riste, T., 1970, Nucl. Instrum. Methods **86,** 1.
Riste, T., E. J. Samuelsen, K. Otnes, and J. Feder, 1971, Solid State Commun. **9,** 1455.
Shapiro, S. M., J. D. Axe, G. Shriane, and T. Riste, 1972, Phys. Rev. B **6,** 4332.
Shapiro, S. M., and N. J. Chesser, 1972, Nucl. Instrum. Methods **101,** 183.
Shirane, G., and J. D. Axe, 1971, Phys. Rev. B **4,** 2957.
Shirane, G., J. D. Axe, J. Harada, and A. Linz, 1970, Phys. Rev. B **2,** 3651.
Shirane, G., J. D. Axe, J. Harada, and J. P. Remeika, 1970, Phys. Rev. B **2,** 155.
Shirane, G., J. D. Axe, and S. M. Shapiro, 1973, Solid State Commun., **13,** 1893.
to be published.
Shirane, G., and V. J. Minkiewicz, 1970, Nucl. Instrum. Methods **89,** 109.
Shirane, G., V. J. Minkiewicz, and A. Linz, 1970, Solid State Commun. **8,** 1941.
Shirane, G., R. Nathans, and V. J. Minkiewicz, 1967, Phys. Rev. **157,** 396.
Shirane, G., R. Pepinsky, and B. C. Frazer, 1956, Acta Crystallogr. **9,** 131.
Shirane, G., and Y. Yamada, 1969, Phys. Rev. **177,** 858.
Skalyo, J. Jr., B. C. Frazer, and G. Shriane, 1970, Phys. Rev. B **1,** 278.
Slater, J. C., 1941, J. Chem. Phys. **9,** 16.
Slater, J. C., 1950, Phys. Rev. **78,** 748.
Unoki, H. and T. Sakudo, 1967, J. Phys. Soc. Jap. **23,** 546.
Yamada, Y., M. Mori, and Y. Noda, 1972, J. Phys. Soc. Jap. **32,** 1565.
Yamada, Y. Y. Noda, J. D. Axe, and G. Shirane, 1974, Phys. Rev., to be published.
Yamada, Y., G. Shirane, and A. Linz, 1969, Phys. Rev. **177,** 848.
Yamada, Y., H. Takatera, and D. L. Huber, 1974, J. Phys. Soc. Jap., **36,** 641.